Vol 10 Suppl., July 2001
1009-1963/2001/10(Suppl.)/00S4-06
Chinese Physics
© 2001 Chin. Phys. Soc.
and IOP Publishing Ltd

RESONANT ANDREEV REFLECTION IN HYBRID SUPERCONDUCTING-NORMAL NANOSTRUTURES*

LIN TSUNG-HAN(林宗涵)
State Key Laboratory for Mesoscopic Physics Department of Physics, Peking University, Beijing 100871, *China*

(Received 11 February 2001)

After a brief description of hybrid superconducting-normal nanostructures and a brief introduction of the Andreev reflection, we present a theoretical investigation of the electron tunneling through a normal-metal/quantum-dot/superconductor (N-QD-S) system where multiple discrete levels of the QD is considered. By using the nonequilibrium-Green- function (NGF) method, the current I is obtained and studied in detail. We find that the Andreev tunneling shows clear resonant behavior, as obtained in previous works. Moreover, the current I versus the gate voltage V_g exhibits different kinds of peaks, depending on the bias voltage, the level-spacing of the QD, and the energy gap of the superconducting electrode. Besides, in I-V characteristics extra peaks superimposed on the conventional current plateaus emerge, which stem from the resonant Andreev reflections.

Keywords: transport properties, tunneling phenomena
PACC: 7430F, 7450

I. INTRODUCTION

Since early 1990s, the tremendous development of the nanofabrication technology has made it possible for manufacturing various hybrid superconducting-normal (S-N) structures, leading to the emergence of a very active research field. As a review of the achievements of early 1990s, the International Symposium on "Mesoscopic Superconductivity " was held in Karlsruhe, Germeny in 1994.[1]

What is interesting in hybrid S-N nanostrutures? It is well known that the essential fearture of mesoscopics is the phase coherence of carriers, electrons or holes; while the superconductivity is a macroscopic quantum condensate with the coherence of Cooper pairs. How these two coherence effects couple with each other? The key mechanism is Andreev reflection, which causes the interplay of the above two kinds of coherences possible, and makes this new field of the condensed matter physics a very fruitful one. It was proposed by Andreev [2] that an electron is reflected from N-S interface in a peculiar way. Because of the energy gap of the superconductor, an electron incoming from normal metal with an energy ϵ below the gap is forbidden to enter the superconductor. However, the incoming electron with the energy ϵ and up-spin may pick up an electron with the energy $-\epsilon$ and down-spin, both entering into the superconductor and forming a Cooper pair; meanwhile a hole with a up-spin is left and going back to the normal metal. Although Andreev reflection is a second order process, it dominates for the clean N-S interface at low temperatures and small bias, since the conventional first order processes are forbidden.[3,4]

II. MAIN PROPERTIES OF ANDREEV REFLECTION

The basic properties of Andreev reflection (AR) are: (1) Retro-reflection: the group velocities of the incident electron and Andreev reflected hole are in opposite directions (perfect only for the electron incoming at the Fermi level). (2) AR is a two-particle process, by which the normal current in N is converted into supercurrent in S. (3) AR is a phase coherent process: the Andreev reflected hole(electron) carries phase information both from the incident elctron(hole) and from the the superconductor.[3,4]

Because the combination of mesoscopics and superconductivity, a number of novel and interesting effects appear, including the quantization of the maximum supercurrent of the superconducting quantum point contacts (SQPC); the enhanced conductance oscillations in Aharonov-Bohm ring with superconducting "mirrors"; the enhanced shot noise in N-S junctions; the AR bound states in SNS structures; the even-odd asymmetry in N-SQD-N and S-SQD-S sys-

*Project supported by the Visiting Scholar Foundation of Key State Laboratory for Mesoscopic Physics in Peking University and by National Natural Science Foundation of China (Grant No.10074001).

tems; the supercurrent control and reverse in SNS; the nonequilibrium and proximity effects in systems with ferromagnetic elements; the hybrid systems with carbon nanotube; etc.[1,3–9]

Works we have done for mesoscopic hybrid S-N structures include: (1) For the electron transport through a mesoscopic hybrid multiterminal resonant-tunneling system which contains a normal central region coupled to multiple superconducting leads, a general expression of the current is derived. This formula can be used to describe the case with time-dependent external fields applied to any parts of the system, arbitrarily finite voltages, and any kinds of interactions in the central region;[10] (2) Resonant Andreev reflection in a N-QD-S system;[11] (3) Photon-assisted Andreev tunneling through a mesoscopic system;[12] (4) Control of the supercurrent in a four-terminal Josephson junction;[13] and some others.

Here we only present our theoretical investigation for the electron tunneling through a N-QD-S structure, a normal quantum-dot connected to two leads, one is a normal metal and the other is a superconductor. Different from Refs.[14] and [15] where only a single level of the QD has been considered, here we assume that the QD has discrete multiple levels, but the intra-dot Coulomb interactions will be neglected for simplicity. Using the nonequilibrium-Green-function(NGF) method, the current formula has been derived. The dependence of the current I upon the gate-voltage, the bias voltage, the level-spacing of the QD, and the energy gap of the superconducting electrode have also been studied in detail.[11,12]

Ⅲ. MODEL AND FORMULATION

We assume that the system under consideration is described by the following Hamiltonian[16,17]

$$H(\tau) = H_{\rm L} + H_{\rm R} + H_{\rm dot} + H_{\rm T}(\tau), \qquad (1)$$

where

$$\begin{aligned} H_{\rm L} =& \sum_{k,\sigma} (\epsilon^0_{{\rm L},k} - ev_{\rm L}) a^\dagger_{{\rm L},k\sigma} a_{{\rm L},k\sigma} \\ H_{\rm R} =& \sum_{p,\sigma} \epsilon^0_{{\rm R},p} a^\dagger_{{\rm R},p\sigma} a_{{\rm R},p\sigma} \\ &+ \sum_{p} \left[\Delta^* a_{{\rm R},p\downarrow} a_{{\rm R},-p\uparrow} + \Delta a^\dagger_{{\rm R},-p\uparrow} a^\dagger_{{\rm R},p\downarrow} \right] \\ H_{\rm dot} =& \sum_{i,\sigma} (\epsilon^0_i - eV_{\rm g}) c^\dagger_{i\sigma} c_{i\sigma}, \qquad (2) \end{aligned}$$

$$\begin{aligned} H_{\rm T} =& \sum_{k,\sigma,i} \left[t_{\rm L} a^\dagger_{{\rm L},k\sigma} c_{i\sigma} + t^*_{\rm L} c^\dagger_{i\sigma} a_{{\rm L},k\sigma} \right] \\ &+ \sum_{p,\sigma,i} \left[t_{\rm R} {\rm e}^{{\rm i}ev_{\rm R}\tau} a^\dagger_{{\rm R},p\sigma} c_{i\sigma} + t^*_{\rm R} {\rm e}^{-{\rm i}ev_{\rm R}\tau} c^\dagger_{i\sigma} a_{{\rm R},p\sigma} \right]. \end{aligned}$$

where $H_{\rm L}$ describes the noninteracting electrons in the left normal-metal lead, $a^\dagger_{{\rm L},k\sigma}$ ($a_{{\rm L},k\sigma}$) are the creation (annihilation) operators of the electron in the left lead, and $v_{\rm L}$ is the voltage of the left lead. $H_{\rm R}$ describes the right superconducting lead with the energy gap Δ. $H_{\rm dot}$ is the Hamiltonian of the quantum dot with multiple discrete energy levels, characterized by the index i and spin σ. For simplicity, the intra-dot electron-electron Coulomb interaction has been neglected. $V_{\rm g}$ is the gate voltage which controls the energy levels in the dot. $H_{\rm T}$ denotes the tunneling part of the Hamiltonian, and t_v ($v = {\rm L}, {\rm R}$) is the hopping matrix and is assumed to be independent of the state k of the leads and the dot-state (i,σ) for simplicity. In order to obtain the Hamiltonian (1) and (2), we have performed a unitary transformation similar to Ref.[16], so that the voltage of the right lead, $v_{\rm R}$, appears as a phase factor in the hopping elements.

Since the current is conserved, it is enough to calculate the current from the left lead to the QD. From the evolution of the total number operator of the electrons in the left lead, $N_{\rm L} = \sum_{k,\sigma} a^\dagger_{{\rm L},k\sigma} a_{{\rm L},k\sigma}$:[18,19]

$$\begin{aligned} I(\tau) =& -e < \dot{N}_{\rm L}(\tau) > \\ =& \frac{{\rm i}e}{\hbar} < [N_{\rm L}, H] > \\ =& \frac{2e}{\hbar} {\rm Re} \sum_{k,i,\sigma} t_{\rm L} \ll c_{i\sigma}(\tau) | a^\dagger_{{\rm L},k\sigma}(\tau) \gg^<, \qquad (3) \end{aligned}$$

where the Green function $\ll A(\tau)|B(\tau') \gg^<$ is defined as: $\ll A(\tau)|B(\tau') \gg^< \equiv i < B(\tau')A(\tau) >$. With the help of Dyson's equation, using the exact Green functions of the electron in the left lead (normal-metal) without the coupling between the dot and the lead, taking a replacement of the sum over k by an integral over energy with the help of the density of states in the left lead, and introducing the linewidth function $\Gamma_{\rm L}(\omega) = 2\pi |t_{\rm L}|^2 \rho_{\rm L}(\omega)$, then Eq.(3) becomes to

$$\begin{aligned} I(\tau) =& -\frac{4e}{\hbar} {\rm Im} \int \frac{{\rm d}\omega}{2\pi} \Gamma_{\rm L} \int_{-\infty}^{\tau} {\rm d}\tau' {\rm e}^{{\rm i}(\omega - ev_{\rm L})(\tau - \tau')} \\ & \cdot \sum_{i,j} \Big[\ll c_{i\uparrow}(\tau) | c^\dagger_{j\uparrow}(\tau') \gg^r f_{\rm L}(\omega) \\ & + \ll c_{i\uparrow}(\tau) | c^\dagger_{j\uparrow}(\tau') \gg^< \Big] \\ \equiv& -\frac{4e}{\hbar} {\rm Im} \int \frac{{\rm d}\omega}{2\pi} \Gamma_{\rm L} \int_{-\infty}^{\tau} {\rm d}\tau' {\rm e}^{{\rm i}(\omega - ev_{\rm L})(\tau - \tau')} \\ & \cdot \left[\boldsymbol{G}^r(\tau,\tau') f_{\rm L}(\omega) + \boldsymbol{G}^<(\tau,\tau') \right]_{11}, \qquad (4) \end{aligned}$$

where $f_{\rm L}(x)=[\exp(x/k_{\rm B}\mathcal{T})+1]^{-1}$ is the Fermi distribution function with $\mathcal{T}$ the temperature, and we have introduced the Nambu representation (2×2 matrix) of the Green functions $\boldsymbol{G}^r(\tau,\tau')$ and $\boldsymbol{G}^<(\tau,\tau')$:[16,20]

$$\boldsymbol{G}^{r,a}(\tau,\tau')\equiv\mp{\rm i}\theta(\pm\tau\mp\tau')\sum_{i,j}\begin{pmatrix} <\{c_{i\uparrow}(\tau),c^\dagger_{j\uparrow}(\tau')\}> & <\{c_{i\uparrow}(\tau),c_{j\downarrow}(\tau')\}> \\ <\{c^\dagger_{i\downarrow}(\tau),c^\dagger_{j\uparrow}(\tau')\}> & <\{c^\dagger_{i\downarrow}(\tau),c_{j\downarrow}(\tau')\}>\end{pmatrix}, \tag{5}$$

$$\boldsymbol{G}^<(\tau,\tau')=i\sum_{i,j}\begin{pmatrix} <c^\dagger_{j\uparrow}(\tau')c_{i\uparrow}(\tau)> & <c_{j\downarrow}(\tau')c_{i\uparrow}(\tau)> \\ <c^\dagger_{j\uparrow}(\tau')c^\dagger_{i\downarrow}(\tau)> & <c_{j\downarrow}(\tau')c^\dagger_{i\downarrow}(\tau)>\end{pmatrix}. \tag{6}$$

After a tedious calculation (details see Refs.[11] and [12]), we finally obtain the following current formula:

$$I=I_A+I_1\ ,$$

with

$$\begin{aligned} I_{\rm A}=&\frac{2e\Gamma_{\rm L}^2}{\hbar}\int\frac{{\rm d}\omega}{2\pi}\left|\tilde{G}^r_{12}\right|^2[f_{\rm L}(\omega+ev_{\rm L}-{\rm e}v_{\rm R})\\ &-f_{\rm L}(\omega-{\rm e}v_{\rm L}+ev_{\rm R})],\end{aligned} \tag{7}$$

$$\begin{aligned} I_1=&\frac{2e\Gamma_{\rm L}\Gamma_{\rm R}}{\hbar}\int\frac{{\rm d}\omega}{2\pi}\tilde{\rho}_{\rm R}(\omega)\Big[\left|\tilde{G}^r_{11}\right|^2+\left|\tilde{G}^r_{12}\right|^2\\ &-\frac{2\Delta}{|\omega|}{\rm Re}\Big[\tilde{G}^r_{11}(\omega)(\tilde{G}^r_{12}(\omega))^*\Big]\Big]\\ &\cdot[f_{\rm L}(\omega+ev_{\rm L}-{\rm e}v_{\rm R})-f_{\rm R}(\omega)].\end{aligned} \tag{8}$$

The formulas of the current, Eqs.(7) and (8), are the central results of this paper. The current I_A represents the contribution from the Andreev reflection. The current I_1 consists of three different processes:[16] (1) The conventional electron tunneling through the system, i.e., the term $\Gamma_{\rm L}\Gamma_{\rm R}\tilde{\rho}_{\rm R}|\tilde{G}^r_{11}(\omega)|^2$; (2) An electron incident from the left lead will convert into a holelike in the right superconducting lead, i.e., the term $\Gamma_{\rm L}\Gamma_{\rm R}\tilde{\rho}_{\rm R}|\tilde{G}^r_{12}(\omega)|^2$, corresponding to a "branch crossing" process in the BTK's theory;[21] (3) An electron (or a hole) incident from the left lead tunnels into the right superconducting lead, picks up a quasi-particle (or a quasi-hole) in the superconductor and creates (or annihilates) a Cooper pair, i.e., the term $-\Gamma_{\rm L}\Gamma_{\rm R}\tilde{\rho}_{\rm R}\frac{2\Delta}{|\omega|}{\rm Re}[\tilde{G}^r_{11}\tilde{G}^{r*}_{12}]$. At zero temperature, if $|eV|<\Delta$ one has $I_1=0$, i.e., only the Andreev reflection process contributes to the current. However, when $|eV|>\Delta$, all of the processes mentioned above make the contributions to the current.

IV. DIFFERENT SERIES OF RESONANT ANDREEV REFLECTION PEAKS

On the basis of the current formulas, Eqs.(7), and (8), we investigate the properties of the current I versus the gate voltage $V_{\rm g}$. Unlike the system of N-QD-N in which the current I versus the gate voltage $V_{\rm g}$ at small bias V exhibits a single series of equally spaced resonance peaks. Now with one of the leads replaced by a superconducting lead, the situation becomes more complicated. In the following we shall discuss in detail two different cases for $eV<\Delta$ and $eV>\Delta$. We set (1) the temperature $\mathcal{T}=0$, (2) the voltage of the right leads $v_{\rm R}=0$ due to the gauge invariance, and carry out all calculations in units of $\hbar=e=1$.

A. The case with $V<\Delta$

In this case only the Andreev reflection current I_A exists. Figure 1 presents I vs $V_{\rm g}$ at different bias. In numerical studies, we have assumed that the QD has 10 discrete levels with equal level-spacing. These levels move downward as $V_{\rm g}$ increases. At small bias, I vs $V_{\rm g}$ exhibits a single series of peaks with equal spacing (marked with "A" in Fig.1(a)). Notice that these resonance peaks are not due to the conventional resonant tunneling, because the conventional tunneling is completely forbidden for $V<\Delta$. Insteadly, these peaks come from the Andreev reflections. When the energy of a state-i of the QD is lined up with the chemical potential of the right superconducting lead, $\mu_{\rm R}$ ($\mu_{\rm R}=-v_{\rm R}$ is set to be zero), then an electron incident from the left lead with the energy $\epsilon=\mu_{\rm R}$ can tunnel into the state-i of the QD, leading to a hole propagating back to the state-i in the QD and the creation of a Cooper pair in the right superconducting lead because of Andreev reflection (see Fig.2(a)). As a result, a current peak emerges in the $I-V_{\rm g}$ curve. Notice that in this Andreev reflection process the incident electron and the reflected hole go through the same state-i of the QD. If the energy level is not lined up with $\mu_{\rm R}$, the Andreev reflection will be very weak, corresponding to a very small Andreev reflection current I_A.

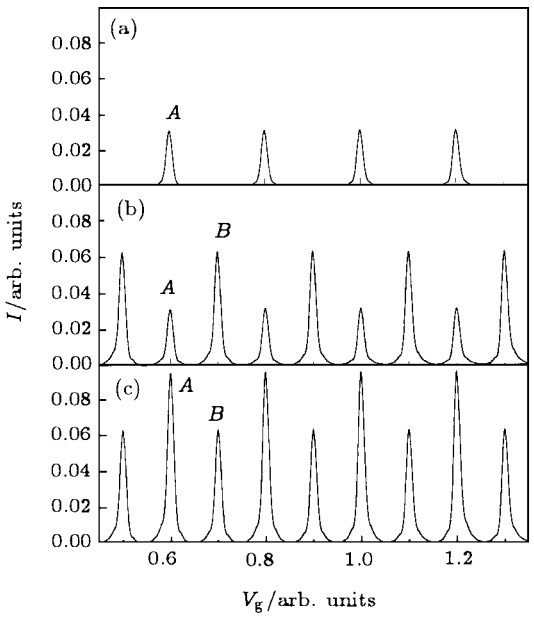


Fig.1. The current I vs the gate voltage V_g for $V < \Delta$. The QD has 10 states with equal level-spacing, $\Delta\epsilon = 0.2$; and $\epsilon_0 = 0$ at $V_g = 0$. Other parameters are chosen as $\Gamma_L = \Gamma_R = 0.01$, $\Delta = 1$. (a), (b), and (c) corresponding to three different bias: $V = 0.02$, 0.15, and 0.25, respectively.

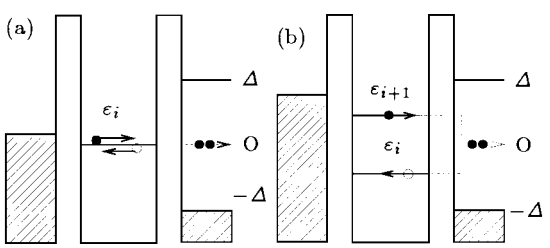


Fig.2. A Schematic diagram for the Andreev reflections: (a) the Andreev reflection through the state-i itself; (b) the Andreev reflection through two states, the state-i and state-$(i+1)$.

Gradually increasing the bias V, the basic feature of I–V_g does not change much, as long as $V < \Delta\epsilon/2$, where $\Delta\epsilon$ is the level-spacing of the QD. Hence the corresponding differential conductance dI/dV is almost zero for $V < \Delta\epsilon/2$. However, when V is greater than $\Delta\epsilon/2$, a series of extra peaks emerges in the I–V_g curve (marked with "B" in Fig.1(b)). The B-type peaks are located in the middle of the A-type peaks with the same peak spacing as that of the A-type peaks, but have much larger amplitudes than that of the A-type peaks (approximately doubled).

The B-type peaks are originated from the following Andreev reflection. For a certain gate voltage V_g, two neighboring states of the QD, say ϵ_i and ϵ_{i+1}, satisfy two conditions: the chemical potential of the right superconducting lead, μ_R, is located in the middle of the two levels; while both of these two levels are below the chemical potential of the left lead, $\mu_L(\mu_L = -v_L)$. So an electron incident with energy $\epsilon = \epsilon_{i+1}$ (or ϵ_i) tunnels from the left lead through the left barrier into the QD's state-$(i+1)$ (or state-i), then Andreev reflected at the right barrier as a hole back to the QD's state-i (or state-$(i+1)$), with a Cooper pair created in the superconductor in the meantime(see Fig.2(b)). Notice that in the B-type Andreev reflection both state-$(i+1)$ and state-i contribute to the current, while the A-type Andreev reflection only involves a single state, so B-type peak has approximately twice the amplitude as that of A-type peak. If $V < \Delta\epsilon/2$, the B-type Andreev reflection can not happen at zero temperature.

When V is less than $\Delta\epsilon$ the amplitude of the A-type peak is smaller than that of the B-type peak. As the bias V is larger than $\Delta\epsilon$ (within the energy range of Γ), the amplitude of the A-type peak becomes larger than that of B-type peak and eventually reaches a height three times it original value (see Fig.1(c)). The positions of A-type peaks do not change. In fact, for a certain gate voltage V_g, a QD's state-i will line up with the chemical potential μ_R, so the Andreev reflection through the state-i itself replaces the original A-type peak. Meanwhile, not only the state-$(i+1)$ and the state-$(i-1)$ are just at $\Delta\epsilon$ and $-\Delta\epsilon$, respectively, both of them are below the left chemical potential μ_L as well, due to the condition $V > \Delta\epsilon$. So the Andreev reflection can also occur through the state-$(i+1)$ and state-$(i-1)$. Now three states $(i-1)$, i, and $(i+1)$ contribute to the A-type peaks, resulting a much higher peak.

In the above numerical calculation, we have assumed that the energy levels in the dot are equal-spacing. If the level-spacing are unequal, the results will be more complicated. Generally, the interval between peaks of each type becomes different from peak to peak. Here we consider a special case of the quantum dot with 10 energy levels and the level-spacig as: $\Delta\epsilon_i = 0.17$ for even i, $\Delta\epsilon_i = 0.23$ for odd i, and $\epsilon_0 = 0$ at $V_g = 0$ ($\Delta\epsilon_i \equiv \epsilon_{i+1} - \epsilon_i$). Figure 3 shows the case of $V > \Delta\epsilon_i$. In contrast to the equal-spacing case (compare to Fig.1(c)), the original A-type peaks are splitted into two peaks (marked with "A_1" and "A_2" in Fig.3). For the unequal level-spacing case, the two peaks from above mentioned two kinds of Andreev reflections no longer overlap completely. So one sees a series of splitted two-peak resonances.

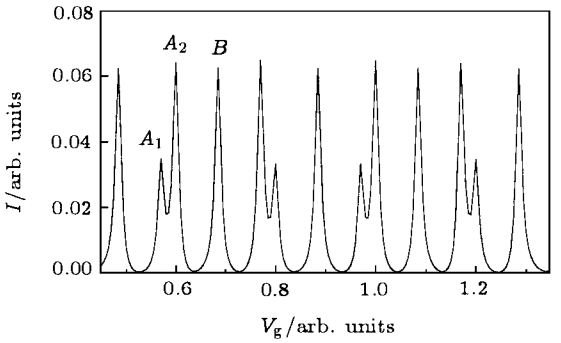


Fig.3. The current I vs the gate voltage V_g for $V < \Delta$. The QD has 10 states but with unequal level-spacing: $\Delta\epsilon_i = 0.17$ for even i, $\Delta\epsilon_i = 0.23$ for odd i, and $\epsilon_0 = 0$ at $V_g = 0$. The other parameters are the same as in Fig.1(c).

In the rest part of this paper, we will keep the assumption of equal level-spacing for simplicity.

B. The case with $V > \Delta$

In the case of $V > \Delta$, all kinds of the processes contribute to the current I, including Andreev reflection and all three kinds of the tunneling processes mentioned above, i.e., both I_A and I_1 are non-zero.

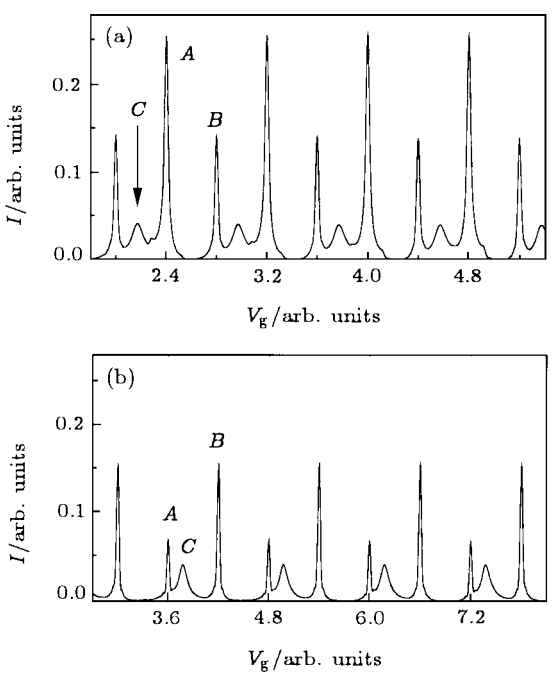


Fig.4. The current I vs the gate voltage V_g for $V > \Delta$. The QD has 10 states with equal level-spacing; and $\epsilon_0 = 0$ at $V_g = 0$. Other parameters are chosen as $\Gamma_L = \Gamma_R = 0.02$, $\Delta = 1$, and $V = 1.04$. (a) and (b) correspond to $\Delta\epsilon = 0.8$ and 1.2, respectively.

Here we studied I–V_g for V slightly larger than Δ (see Fig.4). The difference between Fig.4.(a) and (b) is due to the different level-spacing of the QD's states. Now three series of the peaks emerge in the curve, marked by "A", "B", and "C", respectively, and with the same intervals (or "periods") between the peaks for each series. The positions of the B-type peaks are in the middle of the A-type peaks; and the position of the C-type peak is shifted from the A-type peak by a certain amount which depends on the level-spacing $\Delta\epsilon$ and the gap Δ. The height of the C-type peak is the smallest one.

In the following calculation, we fix the parameters as indicated in Fig.4.(a), and set $\Delta\epsilon = 0.8$. Since $\epsilon_i = \epsilon_i^0 - V_g$ which varies with the gate voltage V_g, the state ϵ_4 is just below the chemical potential μ_L and above the gap Δ when $V_g = 2.2$ (see Fig.5(a)). So the conventional electron and quasi-particle tunneling processes are allowed, leading to the C-type peaks. With the increase of the gate voltage, each level of the QD moves downward. When $V_g = 2.4$, the state ϵ_3 is lined up with the chemical potential μ_R, and the energy difference between the state ϵ_4 or ϵ_2 and μ_R are equal (See Fig.5(b)). So the Andreev reflection can occur through either the state ϵ_3 itself or or other two states ϵ_4 and ϵ_2, leading to the A-type peaks with the largest amplitude (See Fig.4(a)). As V_g is increased further at $V_g = 2.8$, the energy difference between the state ϵ_4 or state ϵ_3 and μ_R are equal (not shown here), and both of ϵ_3 and ϵ_4 are below the chemical potential of the left lead, μ_L. Then the Andreev reflection occurs through the states ϵ_4 and ϵ_3, corresponding to the B-type peaks. For the case with symmetric barriers (as assumed in our calculations), i.e. $\Gamma_L = \Gamma_R$, the maximum probability of the Andreev reflection can reach one, but the conventional transmission probability is less than one because $\Gamma_L \neq \Gamma_R\tilde{\rho}_R$. Therefore the height of the C-type peak is the smallest one.

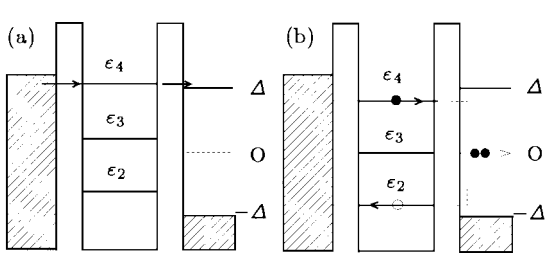


Fig.5. A schematic diagram for the tunneling processes responsible for the C-type and the A-type peaks. (a) and (b) describe the positions of the QD's states, and show the related conventional tunneling(C-type) and the Andreev tunneling(A-type) processes, respectively.

V. THE I–V CHARACTERISTICS

We consider the case in which the levels of the QD vary with the bias V as (for symmetric barriers): $\epsilon_i = \epsilon_i^0 - V/2$. The I–V curve exhibits (figures omitted) extra peaks superimposed on the conventional plateaus. No plateau appears until $V > \Delta$; then plateaus emerge with approximate equal interval. Notice that even for $V < \Delta$ the extra peaks with equal interval due to the Andreev reflections can still emerge. This is because for a certain bias V which satisfies the conditions of the resonant Andreev reflection, the current I increases drastically and a peak emerges. When the bias V is increased slightly, the condition of the resonant Andreev reflection is violated, and hence the current I drops rapidly. The difference of the relative heights of the peaks is determined by the different number of states participating in the resonant Andreev reflections.

VI. CONCLUSIONS

In this paper, we have studied the electron tunneling through the system of a quantum dot with multiple discrete levels and coupled to two leads in which one is superconducting. The resonant behavior and the resonant conditions for Andreev reflection are discussed. The resonant behavior can be clearly seen from I–$V_{\rm g}$. For the N-QD-S system with multiple levels, the I–$V_{\rm g}$ curve has more complicated resonance patterns, with different kinds of peaks, depending on the bias V, the level-spacing of the QD, and the energy gap of the superconducting electrode. From the study of $I-V$ curves we found some extra peaks superimposed on the conventional current plateaus, originated from Andreev reflections.

References

[1] See references in "Mesoscopic Superconductivity", ed. by F. Hekking, G. Schön and D. Averin 1994 *Physics* B **203**

[2] Andreev A F 1964 *Sov. Phys. JETP* **19** 1228

[3] Beenakker C W J 1997 *Rev. Mod. Phys.* **69** 731

[4] Pannetier B and Courtois H, Cond-mat/9912024

[5] Lambert C J and Raimondi R 1998 *J. Phys.:Condens. Matter* **10** 901

[6] Baselmans J J A *et al* 1999 *Nature*(London) **397** 43

[7] Jabob M *et al* 2000 *Appl. Phys. Lett.* **76** 1152

[8] Petrashov V T *et al* Cond-mat/0005437

[9] Morpurgo A F *et al* 1999 *Science* **286** 263

[10] Claughton N R, Leadbeater M and Lambert C J 1995 *J. Phys.: Condens. Matter* **7** 8757

[11] Beenakker C W J 1992 *Phys. Rev.* B **46** 12841

[12] Sun Q F, Wang B G, Wang J and Lin T H 2000 *Phys. Rev.* B **61** 4754

[13] Sun Q F, Wang J and Lin T H 1999 *Phys. Rev.* B **59** 3831

[14] Sun Q F, Wang J and Lin T H 1999 *Phys. Rev.* B **59** 13126

[15] Sun Q F, Wang J and Lin T H 2000 *Phys. Rev.* B **62** 648

[16] Cuevas J C, Martin-Rodero A and Levy Yeyati A 1996 *Phys. Rev.* B **54** 7366

[17] Ishizaka S, Sone J and Ando T 1995 *Phys. Rev.* B **52** 8358

[18] Jauho A P, Wingreen N S and Meir Y 1994 *Phys. Rev.* B **50** 5528

[19] Sun Q F and Lin T H 1997 *J. Phys.:Condens Matter* **9** 4875

[20] Yeyati A L, Martin-Rodero A and Garcia-Vidal F J 1995 *Phys. Rev.* B **51** 3743

[21] Blonder G E, Tinkham M and Klapwijk T M 1982 *Phys. Rev.* B **25** 4515